ORIGINAL RESEARCH

Bioinformatic Analysis on the Prognostic Value of Neurotransmitter Receptor-Related Genes in Kidney Renal Clear Cell Carcinoma

Hao Zhang, MSc; Nan Wang, MSc; Tao Yu, MD; Qingqing Li, MD; Li Yang, MSc; Yang Su, MSc; Peipei Wang, MSc; Juntong Liu, MSc; Luokun Yang, MSc; Jie Zhang, PhD

ABSTRACT

Context • Kidney renal clear-cell carcinoma (KIRC) is a malignant tumor. At an early stage, KIRC patients may experience only mild fever and fatigue or even no symptoms, and these early nonspecific indications can delay treatment. Neurotransmitters and their receptors may be very useful in determining tumorigenesis and predicting metastasis.

Objective • The study intended to investigate the predictive value of neurotransmitter receptor-related genes (NRRGs) using public KIRC data, by determining the biological processes that implicate the prognostic NRRGs and establishing a predictive NR-related risk model, to provide an empirical basis for identifying and treating KIRC patients.

Design • The research team performed a genetic case-control study.

Setting • The study took place at Research Center of Health, Big Data Mining and Applications, Wannan Medical College, Wuhu, China.

Methods • The research team: (1) obtained the transcriptome data related to KIRC from the Cancer Genome Atlas (TCGA) and ArrayExpress databases; (2) developed the differentially expressed NRRGs (DENRRGs) by identifying the NRRGs that intersected with DEGs in KIRC and normal samples; (3) carried out functional enrichment analyses of the DENRRGs; (4) screened the characteristic genes of the DENRRGs using machine learning; (5) created a predictive model using multivariate Cox analyses of the distinctive genes; (6) obtained independent prognostic factors for KIRC patients and established a nomograph model; (7) investigated the sensitivity of KIRC patients to therapeutic agents to examine the variations in immunological features between high-risk and low-risk individuals.

Results • Differential analysis found that 115 NRRGs intersected with 5275 DEGs to provide 52 DENRRGs. Functional enrichment showed that DENRRGs were mainly involved in signal transduction in the nervous system. The machine learning on the 52 DENRRGs filtered out nine characteristic genes. Subsequently, the research team found eight prognostic biomarkers—histamine receptor H2 (HRH2), gamma-aminobutyric acid (GABA) receptor subunit epsilon (GABRE), cholinergic receptor nicotinic delta subunit (CHRND), glutamate receptor ionotropic subunit 2D (GRIN2D), glutamate metabotropic receptor 4 (GRM4), glycine receptor alpha 3 (GLRA3), cholinergic receptor nicotinic beta 4 subunit (CHRNB4), and cholinergic receptor muscarinic-1 (CHRM1)—and established a predictive model. Furthermore, the team precisely predicted the KIRC patients' prognoses using a nomogram that combined their ages, risk scores, and M stages. The infiltration levels of 21 immune cells also significantly differed between the high-risk and low-risk groups, with neutrophils having a significant positive correlation with GABRE and HRH2 and a significant negative correlation with CHRNB4 and GRM4. Finally, the 50% inhibitory concentration (IC50) values for various drugs, such as 5-aminoimidazole-4-carboxamide-1-β-D-ribofuranoside (AICAR), 8-hydroxy-7-(6-sulfonaphthalen-2-yl) diazenyl-quinoline-5-sulfonic acid (NSC-87877), Sunitinib, c-Jun N-terminal kinase (JNK) inhibitor VIII, and tanespimyci (X17. AAG) were significantly lower for high-risk group.

Conclusions • By studying the relevance of biomarkers to the immunological microenvironment of KIRC, the current research team was able to propose a new predictive model for KIRC based on NRRGs, to offer a novel viewpoint for investigating KIRC. The study's results suggest new avenues for research into the pathophysiology and therapy of KIRC. Determining the precise molecular processes by which predictive biomarkers regulate KIRC requires further evidence and analysis. (*Altern Ther Health Med.* 2023;29(8):356-365).

Hao Zhang, MSc, Associate Professor, School of Medicine Information, and Associate Professor, Research Center of Health, Big Data Mining and Applications, Wannan Medical College, Wuhu, China. **Nan Wang,** MSc, Associate Professor, School of Medicine Information, and Associate Professor, Research Center of Health, Big Data Mining and Applications, Wannan Medical College, Wuhu, China. **Tao Yu,** MD, Professor, Yijishan Hospital, Wannan Medical College, Wuhu, China. **Qingqing Li,** MD, Lecturer, School of Medicine Information, and Lecturer, Research Center of Health, Big Data Mining and Applications, Wannan Medical College, Wuhu, China. **Li Yang,** MSc, Associate Professor, School of Medicine Information, and Associate Professor, Research Center of Health, Big Data Mining and Applications, Wannan Medical College, Wuhu, China. **Yang Su,** MSc, Lecturer, School of Medicine Information, and Lecturer, Research Center of Health, Big Data Mining and Applications, Wannan Medical College, Wuhu, China. **Peipei Wang,** MSc, Lecturer, School of Medicine Information, and Lecturer, Research Center of Health, Big Data Mining and Applications, Wannan Medical College, Wuhu, China. **Juntong Liu,** MSc, Lecturer, School of Medicine Information, and Lecturer, Research Center of Health, Big Data Mining and Applications, Wannan Medical College, Wuhu, China.**Luokun Yang,** MSc, Assistant, School of Medicine Information, and Assistant, Research Center of Health, Big Data Mining and Applications, Wannan Medical College, Wuhu, China. **Jie Zhang, PhD**, Associate Professor, Anhui Engineering Research Center of Medical Big Data Intelligent System, Anhui Normal University, Wuhu, China.

Corresponding author: Jie Zhang, PhD
E-mail: zhangjie_ahnu@sina.com

Renal cell carcinoma (RCC) is one of the most cancerous tumors that can develop in the urinary tract.[1] The most prevalent subtype of RCC, accounting for approximately 80%, is kidney renal clear cell carcinoma (KIRC).[2] At an early stage, KIRC patients may experience only mild fever and fatigue or even no symptoms, but at a late stage, cystic degeneration, calcification, necrosis, and hemorrhage, contributing to lower back pain and hematuria, can significantly impair their quality of life (QoL).[3,4]

Treatment

KIRC treatment still depends on surgery.[3,5] However, metastasis causes a poor prognosis with around a third of KIRC patients experiencing metastasis at the time of diagnosis and 25% developing metastases after therapy.[2,6] Mining novel markers for prognostic prediction and individualized therapeutic strategies have important clinical implications in KIRC.

Neurotransmitter Receptors (NRs)

Neurotransmitters, which peripheral and autonomic nerves secrete, regulate pathological and physiological functions by binding to their receptors.[7] According to Jiang et al and Wang et al, cancer cells also produce and secrete neurotransmitters, and their receptors appear on nearly every surface of cancer cells.[7, 8] Those researchers also found that the NR-mediated signaling pathways that regulate immune response are critical for carcinogenesis.

Wang et al found that NRs are an essential nervous system component in the body's physiological and pathological processes and that tumor cells broadly express NRs, which modulate the tumor microenvironment, angiogenesis, metastasis, and proliferation.[8] Jiang et al and Schuller found that neurotransmitters and their receptors are closely related to cell proliferation, apoptosis, metastasis and cancer-related angiogenesis in non-small cell lung cancer, glioblastoma, pancreatic cancer and breast cancer.[8-12]

In KIRC, Virginia et al showed that the beta 2-adrenergic receptor (ADRB2) regulated the inflammatory response and oxidative stress of KIRC cells.[13] Tung et al found that antagonists targeting dopamine receptors (DRs) could inhibit the growth of KIRC cells.[1] Lee et al found that the receptor of γ-aminobutyric acid (GABA) can act as a prognostic marker in KIRC.[14]

By controlling the transmembrane transfer of water, urea, glycerol, and other ions, aquaporins may also influence the prognosis for KIRC.[15]The ionophore gramicidin A can disrupt the transmembrane potential of KIRC cells by making the cell membrane permeable to specific ions and is associated with angiogenesis, cell death and growth of KIRC.[16, 17]

Although the above few studies have demonstrated the critical function of NRs in KIRC development, extensive research on NRs' prognostic significance in KIRC remains lacking. Thus, a comprehensive and systematic study of neurotransmitter receptor-related genes (NRRGs) in the prognosis of KIRC could be of great significance.

Possible Predictive Biomarkers

Possible biomarkers in KIRC include: (1) histamine receptor H2 (HRH2), (2) glutamate metabotropic receptor 4 (GRM4), (3) cholinergic receptor nicotinic beta 4 subunit (CHRNB4), (4) cholinergic receptor muscarinic-1 (CHRM1), (5) gamma-aminobutyric acid (GABA) receptor subunit epsilon (GABRE), (6) cholinergic receptor nicotinic delta subunit (CHRND), (7) glutamate receptor ionotropic subunit 2D (GRIN2D), and (8) glycine receptor alpha 3 (GLRA3).

HRH2. Xie et al identified HRH2 as a dysregulated, epigenetic, protein-coding gene and found that it's a prognostic biomarker.[18]

GRM4. Huang et al found that GRM4, a metabotropic glutamate receptor, can inhibit cyclic adenosine monophosphate (cAMP) production and protein kinase A (PKA) by negatively coupling to adenylyl cyclase.[19] Bai reported that GRM4 is related to KIRC prognosis, but the specific mechanism remains unclear.[20]

CHRNB4 and CHRM1. Meixner et al found that CHRNB4 and CHRM1 are acetylcholine receptors in vascular remodeling in chronic, renal allograft injury.[21] Other studies have found that CHRNB4 is involved in lung cancer[22] and head and neck cancer,[23] while CHRM1 is involved in glioma[24] and colon cancer.[25]

GABRE. Although researchers have established little about its role in KIRC, some studies have linked GABRE to migraines, colon cancer, and non-small cell lung cancer (NSCLC).[26-28]

CHRND. Some studies have found that CHRND, a gene encoding the muscle acetylcholine receptor, is associated with myasthenia,[29] neuromuscular diseases,[30] and head and neck squamous cell carcinomas (HNSCCs).[31]

GRIN2D. Ferguson et al found that GRIN2D can stimulate intracellular calcium inflow.[32] Moreover, Ferguson et al and other studies have found that GRIN2D is closely related to endothelial function, angiogenesis, and DNA methylation in tumors and acts as the biomarker for colorectal cancer, pancreatic ductal adenocarcinoma, liver cancer, and Parkinson's disease.[32-36]

GLRA3. Some studies have found that GLRA3 is a chloride channel gate and is involved in small-cell lung cancer,[37] diabetic nephropathy,[38] and leukemia.[39]

Inflammatory Cells

Roussel et al found that neutrophils, inflammatory cells in the tumor microenvironment, are crucial to the development of tumors,[40] and Quan and Huang found that they have a close relationship with prognosis for KIRC.[41]

Roussel et al and Cordeiro et al found that a prognostic factor for KIRC patients may be the neutrophil-to-lymphocyte ratio.[40, 42] In addition, Shi et al detected a high expression of HRH2 in neutrophils of mouse intestinal tissue and found that HRH2 regulates the infiltration and differentiation of neutrophils for inflammation and colon-tumor sites.[43]

Current Study

The current study intended to investigate the predictive value of NRRGs using public KIRC data, by determining the biological processes that implicate the prognostic NRRGs and establishing a predictive NR-related risk model, to provide an empirical basis for identifying and treating KIRC patients.

METHODS

Procedures

The research team performed a genetic case-control study, which took place at Research Center of Health, Big Data Mining and Applications, Wannan Medical College, Wuhu, China.

Data collection. The research team obtained the KIRC-related transcriptome data, which included 526 KIRC and 72 normal reference samples, from the Cancer Genome Atlas (TCGA) database.[44] Of these, 522 KIRC samples had complete survival and clinical information. The team included 101 KIRC samples with unique survival data in an external validation set, the E-MTAB-1980 dataset, extracted from the ArrayExpress database,[45] and then obtained 115 NRRGs from the available reports.[8]

Identification and functional enrichment analysis of differentially expressed NRRGs (DENRRGs). The research team extracted the differentially expressed genes (DEGs) for the normal and KIRC samples from the TCGA-KIRC platform using the limma R software package.[46, 47] (Walter and Eliza Hall Institute of Medical Research, Melbourne, Victoria, Australia).

To demonstrate the filtering results, the team used the ggplot2 R tool, version 3.3.5, to construct a volcano plot[48] and displayed the DEG expression on a heat map generated using the pheatmap R package, version 1.0.12.[49] The team: (1) then estimated the distribution of the KIRC and normal samples using (PCA) analysis of samples from the TCGA-KIRC dataset based on the DEGs; (2) next obtained the DENRRGs by finding the intersection of DEGs and NRRGs using jvenn; (3) using the Database for Annotation, Visualization, and Integrated Discovery (DAVID) platform,[50] then examined the DENRRGs employing Gene Ontology (GO)[51] and Kyoto Encyclopedia of Genes and Genomes (KEGG) analysis.[52-54] analysis.

Identification of predictive biomarkers. Random forest is a method of training a large number of survival trees and weighting the final prediction from the individual trees in the form of voting. The research team: (1) performed the random forest analysis using RandomForestSRC package's[55] (University of Miami, Florida, USA). rfsrc function to acquire prognosis-related genes based on DENRRGs and survival information in the TCGA-KIRC database[56]; (2) identified the importance ranking of each gene by setting parameters—ntree = 1000 and "na.action = na.impute; and (3) filtered the candidate prognostic genes according to an importance threshold importance of >0.3.

The team also performed a "least absolute shrinkage and selection operator" (LASSO) analysis on the DENRRGs using the glmnet package in the R software, version 4.0-2, to identify the prognosis-related genes.[57] The team: (1) used the intersection identifying the prognosis-related genes, as obtained from the above two algorithms, to acquire the characteristic genes, and (2) performed a multivariate stepwise Cox analysis of the distinct genes using the step function, and (3) obtained the predictive biomarkers by setting the parameter to direction = both.[58]

Evaluation and confirmation of prognostic model's accuracy. Based on the median risk score, the research team: (1) categorized the patients with KIRC in the TCGA-KIRC dataset into high-risk and low-risk groups, with 261 patients each[59]; (2) compared the two groups' survival rates using a Kaplan-Meier (K-M) analysis[60]; (3) plotted the predictive model's receiver operator characteristic (ROC) curves using the survivalROC R tool[60]; and (4) assessed the distribution of the samples in the two groups using PCA. The team subsequently verified the prediction model's reliability in an external validation set.

Development of the nomograph model. The research team: (1) used multifactorial and univariate Cox analyses for the TCGA-KIRC dataset to identify independent predictive variables for KIRC based on clinical features and risk scores[61,62]; (2) then combined components having independent predictive value to produce a nomogram model, and (3) determined the accuracy of the nomogram model through decision curve analysis (DCA), calibration curves, and ROC curves.[60]

The immune infiltration landscape. The research team: (1) determined the abundance of 28 immune cells in the samples from the TCGA-KIRC dataset, using single-sample gene set enrichment analysis (ssGSEA)[63]; (2) compared the distributions of immune cells in samples from different risk groups using the Wilcox.test and presented them in a box plot employing the R package ggplot2.[64] The team used the ggplot2 R software to develop a lollipop plot to show the association between biomarkers and differently infiltrating immune cells.[64]

Prediction of drug responsiveness. The research team: (1) applied the pRRophetic R package to determine the 50% inhibitory concentration (IC50) values for 138 drugs using samples from various risk groups from the Genomics of Drug Sensitivity in Cancer (GDSC) database[65, 66]; and (2) visualized them by plotting box plots with the R package ggplot2.[67]

RESULTS

DENRRGs and Signal Transduction

Through differential analysis, the research team screened 5275 DEGs—2392 upregulated and 2883 downregulated—from the normal and KIRC samples in the TCGA-KIRC dataset, using an adjusted $P < .05$ and a |log2fold change (FC)| >1 (Figures 1A and 1B). Based on the DEGs, the PCA analysis of the samples from the TCGA-KIRC dataset was able to create distinctions between the standard and KIRC samples (Figure 1C). Furthermore, the research team obtained 52 DENRRGs by creating the intersection between the 5275 DEGs of the normal and KIRC samples and 115 NRRGs (Figure 1D).

The GO analysis suggested that the DENRRGs had an important role in transmitting chemical synapses, postsynaptic excitability potentials, ions transport across membranes, neurological processes, and modulation of membrane potential (Figure 1E). The KEGG analysis suggested that the DENRRGs had an important role in creating interactions in neuroactive ligands with receptors, glutamatergic synapses, nicotine and morphine addiction, retrograde endocrine hormone signaling, and GABAergic synapses (Figure 1F).

Figure 1. Identification and Analysis of the DEGs Between the Normal and KIRC Samples in the TCGA-KIRC Dataset. Figures 1A and 1B show a volcano plot and heatmap, respectively, of the 5275 DEGs with |log2fold change (FC)| >1 and adj. $P < .05$. Figure 1C shows the PCA for the TCGA-KIRC cohorts according to the expression of DEGs. Figure 1D shows the Venn diagram of the 52 DENRRGs. Figure 1E shows the most enriched GO terms of the 52 DENRRGs. Figure 1F shows the mainly enriched KEGG pathways of 52 DENRRGs.

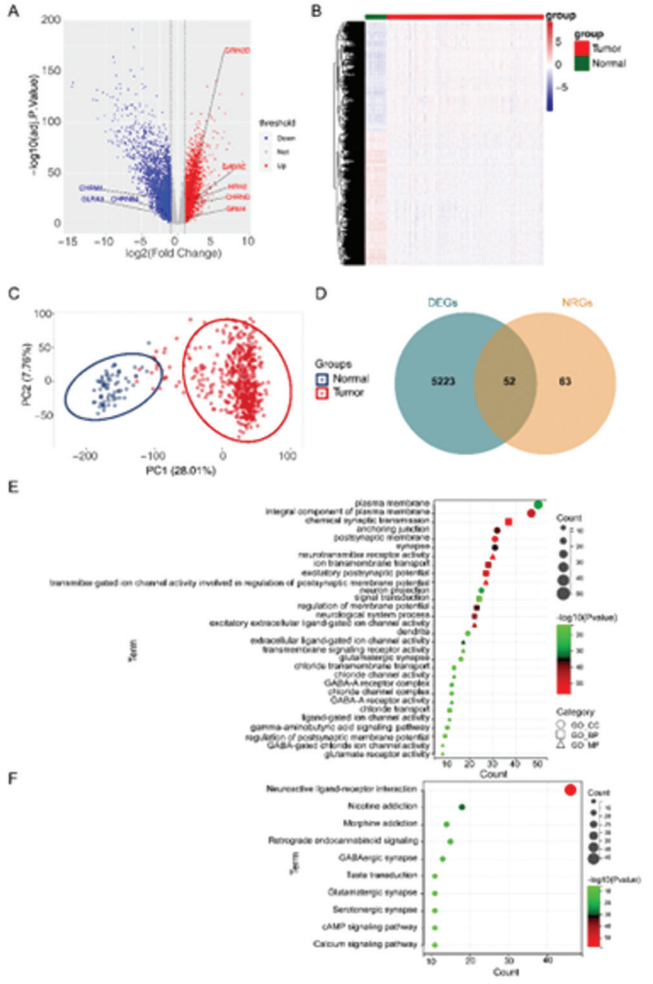

Abbreviations: DEGs, differentially expressed genes; DENRRGs, differentially expressed NRRGs; GO, gene ontology; KEGG, Kyoto Encyclopedia of Genes and Genomes; KIRC, kidney renal clear cell carcinoma; NRRGs, neurotransmitter receptor-related genes; PCA, principal component analysis; TCGA, The Cancer Genome Atlas.

Figure 2. Screening for the Prognostic Biomarkers. Figure 2A shows the random forest survival analysis for the DENRRGs. Figure 2B shows the 12 genes identified as prognosis-related genes with a relative variable importance of >0.3. Figure 2C shows the 16 prognosis-related genes selected using the LASSO Cox models. Figure 2D shows the cross-validation for the tuning parameter selection in the LASSO model. Figure 2E shows the Venn diagram of nine characteristic genes through two algorithms. Figure 2F shows the multivariate stepwise Cox analysis to identify the prognostic biomarkers based on the distinct genes.

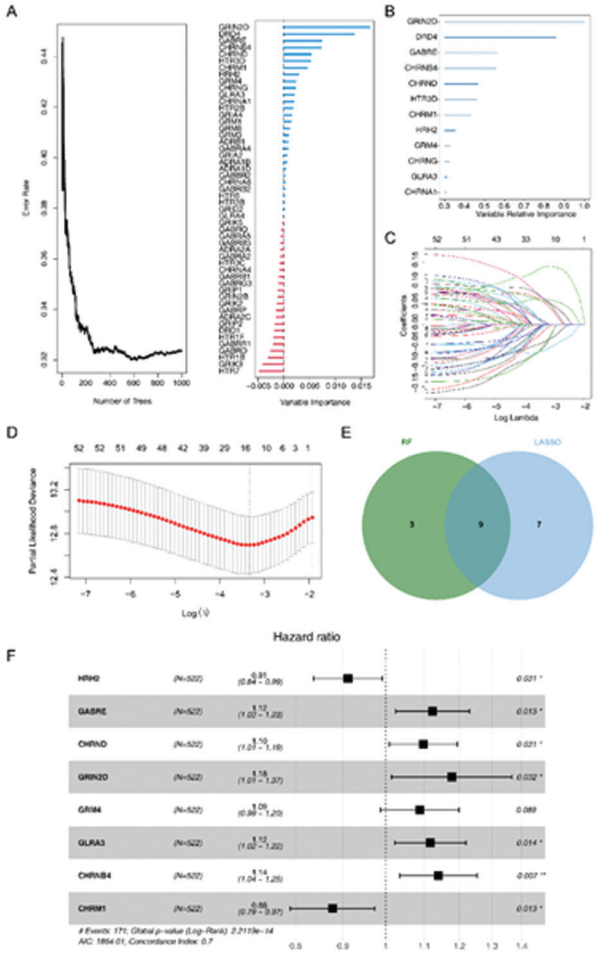

Abbreviations: DENRRGs, differentially expressed NRRGs; LASSO, least absolute shrinkage and selection operator.

Predictive Biomarkers

Figures 2A and 2B show the random forest survival analysis of DENRRGs in the TCGA-KIRC dataset, which yielded 12 prognosis-related genes: (1) GRIN2D, (2) dopamine receptor D4 (DRD4), (3) GABRE, (4) CHRNB4, (5) CHRND, (6) 5-hydroxytryptamine receptor 3D (HTR3D), (7) CHRM1, (8) HRH2, (9) GRM4, (10) cholinergic receptor nicotinic gamma subunit (CHRNG), (11) GLRA3, and (12) cholinergic receptor nicotinic alpha 1 subunit (CHRNA1).

Figures 2C and 2D show the LASSO regression analysis, which revealed 16 prognosis-related genes (lambda.min=0.03550206), including: (1) GABA receptor subunit delta (GABRD), (2) HRH2, (3) GABRE, (4) CHRND, (5) GABA type A receptor subunit theta (GABRQ), (6) DRD4, (7) GRIN2D, (8) GRM4, (9) adrenoceptor alpha 1D (ADRA1D), (10) GLRA3, (11) GABA type A receptor subunit beta3 (GABRB3), (12) CHRNB4, (13) CHRM1, (14) GABA A receptor, subunit gamma 3 (GABRG3), (15) GABA type A receptor subunit Pi (GABRP), and (16) glutamate metabotropic receptor 1 (GRM1).

Then, the team obtained the nine characteristic genes—GRIN2D, DRD4, GABRE, CHRNB4, CHRND, CHRM1,

HRH2, GRM4, and GLRA3—by determining the intersection of the 12 prognosis-related genes from the random forest survival analysis and the 16 prognosis-related genes obtained from the LASSO regression analysis (Figure 2E).

The team then constructed and used the predictive model, finding eight predictive biomarkers—HRH2, GABRE, CHRND, GRIN2D, GRM4, GLRA3, CHRNB4, and CHRM1—using a multifactorial Cox regression analysis of the nine characteristic genes (Figure 2F).

Reliability of Prognostic Model

The KIRC patients were divided into the high- and low-risk score groups based on the medium value of the risk score (0.963915812) (Figure 3A). The expression of HRH2 and CHRM1 was lower in the high-risk group, while the expression of GABRE, CHRND, GRIN2D, GRM4, GLRA3, and CHRNB4 was higher than that of the low-risk group (Figure 3B).

Figure 3C shows that the survival duration for the high-risk group was significantly lower than that of the low-risk group ($P < .000s1$). The risk score was a reliable predictor of patients' survival; the AUCs for the KIRC patients' risk scores were 0.747, 0.69, and 0.737 for survival for 1, 3, and 5 years, respectively. (Figure 3D). Thus, the PCA analysis using biomarkers may adequately characterize the samples' distribution (Figure 3E).

The research team then used the external validation set to verify the predictive model's accuracy. KIRC patients with the survival status of "Dead" were predominantly seen in the high-risk group (Figure 3F). HRH2 and CHRM1 expression was lower in the high-risk group than in the low-risk group, while the rest of the biomarkers were the reverse (Figure 3G).

Figure 3H shows that the high-risk group's survival probability, according to the K-M survival curves analysis, was significantly lower than that of the low-risk group ($P = .01$). AUCs of 0.755, 0.662, and 0.709 for the risk scores predicting survival at 1, 3, and 5 years for KIRC patients, respectively, indicated that the risk score could accurately predict patients' survival in the external validation set (Figure 3I). The PCA analysis based on biomarkers also could accurately describe the distribution of samples in the external validation set (Figure 3J).

Figure 3. Construction and Assessment of the Predictive Model in KIRC. Figure 3A shows the distribution of the risk scores and survival statuses of KIRC patients for the two risk groups, stratified by the predictive model in the TCGA-KIRC cohorts. Figure 3B shows the gene expression heatmap of the prognostic biomarkers between for the two risk groups. Figure 3C shows the K-M survival analysis of the two risk groups in the TCGA-KIRC cohorts ($P < .0001$). Figure 3D shows the ROC curves for the predictive accuracy of the prognostic model in the TCGA-KIRC cohorts. Figure 3E shows the PCA plot between the high- and low-risk groups in the TCGA-KIRC cohorts. Figure 3F shows the distribution of the risk scores and survival statuses of KIRC patients for the two risk groups, stratified by the predictive model in the E-MTAB-1980 dataset. Figure 3G shows the gene expression heatmap of prognostic biomarkers between the two risk groups in the E-MTAB-1980 dataset. Figure 3H shows the K-M survival analysis of the two risk groups in the E-MTAB-1980 dataset (p=0.01). Figure 3I shows the ROC curves for the predictive accuracy of the prognostic model in the E-MTAB-1980 dataset. Figure 3J shows the PCA plot between the high- and low-risk groups in the E-MTAB-1980 dataset.

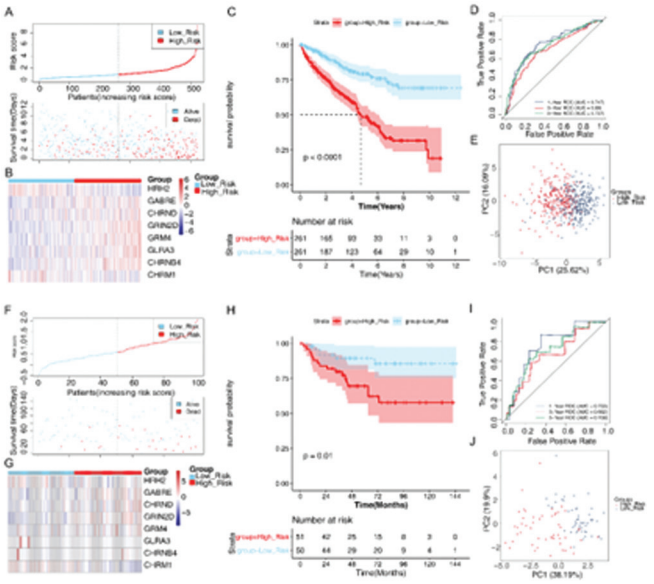

Note: Figure 3C $P < .0001$, indicating that survival duration for the high-risk group was significantly lower than that of the low-risk group, Figure 3H $P = .01$, indicating that survival probability for the high-risk group was significantly lower than that of the low-risk group

Abbreviations: K-M, Kaplan-Meier; KIRC, kidney renal clear cell carcinoma; PCA, principal component analysis; ROC, receiver operator characteristic; TCGA, The Cancer Genome Atlas.

Nomogram Model

Age ($P < .001$), risk score ($P < .001$), tumor stage ($P < .001$), histological neoplasm grade ($P < .001$), M stage ($P < .001$), T stage ($P < .001$), and N stage ($P < .001$) were all associated with KIRC patients' survival in the TCGA-KIRC dataset, as determined using univariate Cox analysis (Figure 4A). Figure 4B shows the independent prognostic value of M stage ($P = .032$), age ($P = .019$), and risk score ($P < .001$), identified using multifactorial Cox analysis.

Estimating KIRC patients' prognosis reliably was possible by fusing the M stage, age, and risk score to create a nomogram model (Figures 4C and 4D). The ROC curves indicated that the nomogram model could accurately predict the prognosis of KIRC patients at years 1, 3, and 5 (Figure 4E). The data from the DCA curves showed that the nomogram model provided better therapeutic value than other independent predictive indicators (Figure 4F).

Biomarkers and Immune Cells

Because the prognosis of tumors was intimately interrelated to the immune microenvironment, the research

Figure 4. Establishment and Assessment of the Nomogram Based on the Risk Score. Figures 4A and 4B show the univariate and multivariate Cox regression analyses, which confirmed that the risk score could be an independent prognostic factor affecting the prognosis of KIRC patients. Figure 4C shows the nomogram combining risk score and other clinicopathological parameters, which was developed to predict 1-, 3-, and 5-year survival. Figure 4D shows the calibration curves of the nomogram. Figure 4E shows the ROC curve of the nomogram for survival prediction. Figure 4F shows the DCA of the 1-, 3-, and 5-year survival in the TCGA-KIRC dataset.

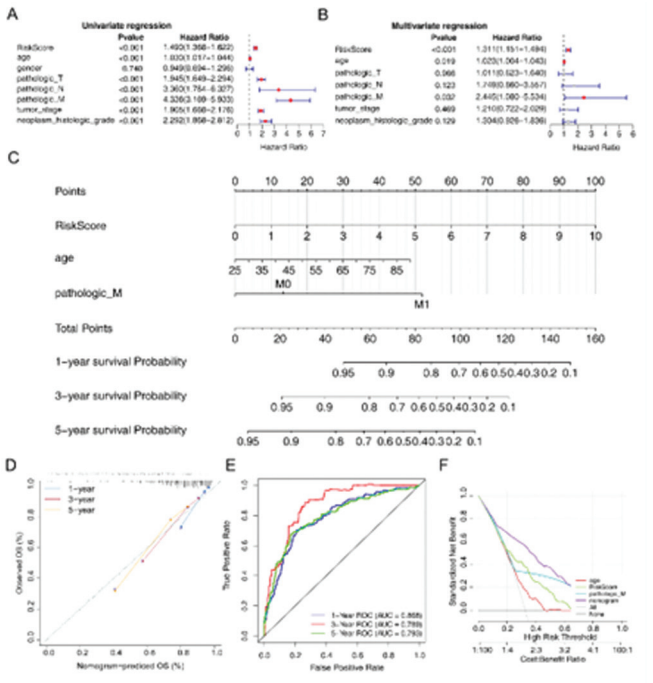

Note: Figure 4A $P < .001$, indicating that age, risk score, tumor stage, histological neoplasm grade, M stage, T stage, and N stage were all associated with KIRC patients' survival, as determined using univariate Cox analysis. Figure 4B $P < .001$, indicating that age, risk score, and M stage had significant independent prognostic value as determined using multifactorial Cox analysis

Abbreviations: DCA, decision curve analysis; KIRC, kidney renal clear cell carcinoma; ROC, receiver operator characteristic; TCGA, The Cancer Genome Atlas.

team also researched the relationship of the prognosis biomarkers and the immune microenvironment in KIRC. Figure 5A shows that the concentration of 21 immune cells in the TCGA-KIRC dataset was significantly different between the high- and low-risk groups ($P < .05$).

In addition, the team further investigated the relevance of the prognostic biomarkers to the differential immune cells. The neutrophil, the activated CD4 T cell, the type 2 T helper cell, the central memory CD4 T cell, the memory B cell, the central memory CD8 T cell, MDSC, macrophage etc., had the most significant correlations with biomarkers.

The neutrophil was significantly positively correlated with GABRE ($P < .0001$, cor = 0.174) and HRH2 ($P < .0001$, cor = 0.256) and negatively correlated with CHRNB4

Figure 5. Immune-related Analyses for the Correlation of Risk Score and Immune Cells. Figure 5A shows the boxplot for the contents of 21 immune cells between the different risk groups in the TCGA-KIRC dataset's Lollipop Chart for the correlation of the significantly different immune cells, Figure 5B shows the CHRM1, Figure 5C the CHRNB4, Figure 5D the CHRND, Figure 5E the GABRE, Figure 5F the GLRA3, Figure 5G the GRIN2D, Figure 5H the GRM4, and Figure 5I the HRH2.

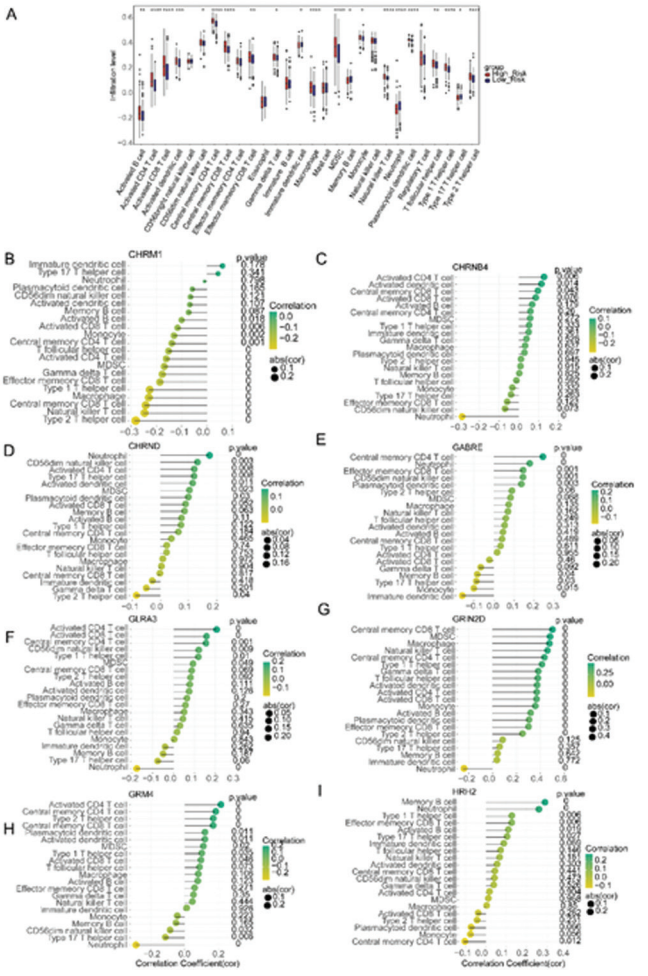

*$P < .05$, indicating that the type 2 T helper cell was significantly negatively correlated with CHRND

****$P < .0001$, indicating that the neutrophil was significantly positively correlated with GABRE and HRH2 and significantly negatively correlated with CHRNB4 and GRM4; that the activated CD4 T cell was significantly positively correlated with GRM4 and GLRA3; and that the type 2 T helper cell was significantly negatively correlated with CHRM1

Abbreviations: CD, cluster of differentiation; CHRM1, cholinergic receptor muscarinic-1; CHRNB4, cholinergic receptor nicotinic beta 4 subunit; CHRND, cholinergic receptor nicotinic delta subunit; GABRE, gamma-aminobutyric acid receptor subunit epsilon; GLRA3, glycine receptor alpha 3; GRIN2D, GluN2D subunit protein; GRM4, glutamate metabotropic receptor 4; HRH2, histamine receptor H2; KIRC, kidney renal clear cell carcinoma; MDSC, myeloid-derived suppressor cells; TCGA, The Cancer Genome Atlas.

($P < .0001$, cor = -0.29) and GRM4 ($P < .0001$, cor = -0.288). The activated CD4 T cell was significantly positively correlated with GRM4 ($P < .0001$, cor = 0.208) and GLRA3 ($P < .0001$, cor = 0.203). Figures 5B to 5I show that CHRM1 and CHRND demonstrated a significant negative correlation with the type 2 T helper cell ($P < .0001$, cor = -0.286 and $P < .05$, respectively).

Thus, the research team considered that the differential immune cells, especially the neutrophil and type 2 T helper cell, might be linked to the occurrence and development of KIRC.

High Risk and Drug Sensitivity

In the different risk groups, 107 drugs showed significantly varying IC50 values ($P < .05$). Figures 6A to 6E show that five drugs among them had the most significant differences: (1) "5-aminoimidazole-4-carboxamide-1-β-D-ribofuranoside" (AICAR), (2) 8-hydroxy-7-(6-sulfonaphthalen-2-yl)diazenyl-quinoline-5-sulfonic acid (NSC-87877), (3) Sunitinib, (4) c-Jun N-terminal kinase (JNK) inhibitor VIII, and (5) tanespimyci (X17.AAG), all $P = <2e\text{-}16$.

Figure 6. Exploration of the Potential Therapeutic Agents for the KIRC Patients With Different Risk Scores. The IC50 values of the most effective drugs were shown, including AICAR (6A), NSC.87877 (6B), Sunitinib (6C), and JNK. Inhibitor.VIII (6D), and X17.AAG (6E).

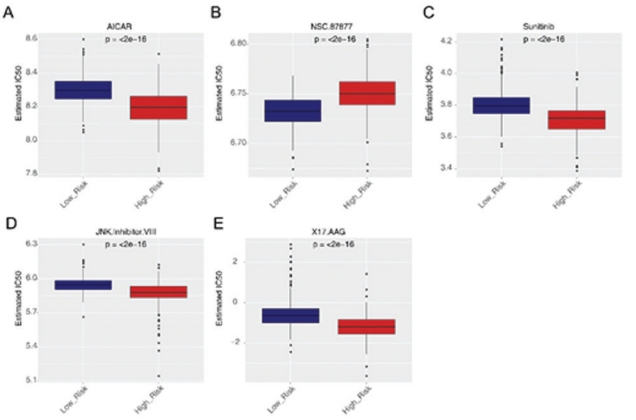

Abbreviations: AICAR, 5-aminoimidazole-4-carboxamide-1-β-D-ribofuranoside; IC50, 50% inhibitory concentration; JNK.Inhibitor.VIII, c-Jun N-terminal kinase (JNK) inhibitor VIII; NSC.87877, 8-hydroxy-7-(6-sulfonaphthalen-2-yl)diazenyl-quinoline-5-sulfonic acid (NSC-87877); X17.AAG, tanespimyci.

DISCUSSION

In the present investigation, the research team established a new KIRC predictive model using NRRGs and examined the underlying biological processes. The current study found 52 DENRRGs may be critical for KIRC development and treatment.

Machine learning in the current study identified HRH2, GABRE, CHRND, GRM4, GLRA3, CHRNB4 and CHRM1 as predictive biomarkers, and the research team constructed the model predicting KIRC prognosis. Further testing found a predictive value for HRH2 and suggested that HRH2 may regulate KIRC via NR-mediated signaling pathways, with CHRNB4, CHRM1, GABRE, CHRND, GRIN2D and GLRA3 having significant prognostic value in KIRC. Furthermore, those eight predictive biomarkers may affect KIRC prognosis by NR-related signaling pathways.

The current study also found that 21 immune cells infiltrated differentially in the two risk groups. Among them, neutrophils were significantly associated with the expressions of GABRE HRH2, CHRNB4, and GRM4. Thus, the research team speculated that HRH2 might regulate KIRC via the infiltration and differentiation of neutrophils. In addition, for the first time in a study, the team found for KIRC that neutrophil infiltration may also be associated with GABRE, HRH2, CHRNB4 and GRM40-mediated signal transduction pathways.The study has certain limitations: (1) Our research was based on analysis of public databases and requires experimental validation; (2) The sample size of the dataset is limited and needs to be expanded further; (3) The effectiveness of the drugs we analyzed needs to be validated in clinical settings, among others.

CONCLUSIONS

By studying the relevance of biomarkers to the immunological microenvironment of KIRC, the current research team was able to propose a new predictive model for KIRC based on NRRGs, to offer a novel viewpoint for investigating KIRC. The study's results suggest new avenues for research into the pathophysiology and therapy of KIRC. Determining the precise molecular processes by which predictive biomarkers regulate KIRC requires further evidence and analysis.

AUTHORS' DISCLOSURE STATEMENT

The Humanities and Social Science Foundation of Anhui Higher Education Institutions of China (SK2020A0379), the Major Quality Engineering Project of Anhui Higher Education Institutions of China (2020ZDXSJG369), the Research Program in Universities of Anhui Province, China (2022AH010073, 2022AH051203), the Key Program for Higher Education Teaching Reform Research of Wannan Medical College (2022JYXM08), and the Scientific Research Project of Wannan Medical College (WK202116, WK202208) funded the study. The authors declare that they have no competing interests.

ACKNOWLEDGMENTS

We would like to thank Fulong Chen (Anhui Engineering Research Center of Medical Big Data Intelligent System) with assistance, for his valuable suggestions with this study.

DATA AVAILABILITY STATEMENT

The study acquired the E-MTAB-1980 data set from the ArrayExpress database and downloaded the publicly accessible datasets of KIRC used in this investigation from the TCGA database.

REFERENCES

1. Tung MC, Lin YW, Lee WJ, et al. Targeting DRD2 by the antipsychotic drug, penfluridol, retards growth of renal cell carcinoma via inducing stemness inhibition and autophagy-mediated apoptosis. *Cell Death Dis*. 2022;13(4):400. doi:10.1038/s41419-022-04828-3
2. Sun Z, Tao W, Guo X, et al. Construction of a Lactate-Related Prognostic Signature for Predicting Prognosis, Tumor Microenvironment, and Immune Response in Kidney Renal Clear Cell Carcinoma. *Front Immunol*. 2022;13:818984. doi:10.3389/fimmu.2022.818984
3. Xiong W, Zhong J, Li Y, Li X, Wu L, Zhang L. Identification of Pathologic Grading-Related Genes Associated with Kidney Renal Clear Cell Carcinoma. *J Immunol Res*. 2022;2022:2818777. doi:10.1155/2022/2818777
4. Ochocki JD, Khare S, Hess M, et al. Arginase 2 Suppresses Renal Carcinoma Progression via Biosynthetic Cofactor Pyridoxal Phosphate Depletion and Increased Polyamine Toxicity. *Cell Metab*. 2018;27(6):1263-1280.e6. doi:10.1016/j.cmet.2018.04.009
5. Zhang G, Chen X, Fang J, Tai P, Chen A, Cao K. Cuproptosis status affects treatment options about immunotherapy and targeted therapy for patients with kidney renal clear cell carcinoma. *Front Immunol*. 2022;13:954440. doi:10.3389/fimmu.2022.954440
6. Hsieh JJ, Purdue MP, Signoretti S, et al. Renal cell carcinoma. *Nat Rev Dis Primers*. 2017;3(1):17009. doi:10.1038/nrdp.2017.9
7. Jiang SH, Hu LP, Wang X, Li J, Zhang ZG. Neurotransmitters: emerging targets in cancer. *Oncogene*. 2020;39(3):503-515. doi:10.1038/s41388-019-1006-0

8. Wang X, Li Y, Shi Y, et al. Comprehensive analysis to identify the neurotransmitter receptor-related genes as prognostic and therapeutic biomarkers in hepatocellular carcinoma. *Front Cell Dev Biol*. 2022;10:887076. doi:10.3389/fcell.2022.887076
9. Wu XY, Zhang CX, Deng LC, et al. Overexpressed D2 Dopamine Receptor Inhibits Non-Small Cell Lung Cancer Progression through Inhibiting NF-κB Signaling Pathway. *Cell Physiol Biochem*. 2018;48(6):2258-2272. doi:10.1159/000492644
10. Dolma S, Selvadurai HJ, Lan X, et al. Inhibition of Dopamine Receptor D4 Impedes Autophagic Flux, Proliferation, and Survival of Glioblastoma Stem Cells. *Cancer Cell*. 2016;29(6):859-873. doi:10.1016/j.ccell.2016.05.002
11. Jandaghi P, Najafabadi HS, Bauer AS, et al. Expression of DRD2 Is Increased in Human Pancreatic Ductal Adenocarcinoma and Inhibitors Slow Tumor Growth in Mice. *Gastroenterology*. 2016;151(6):1218-1231. doi:10.1053/j.gastro.2016.08.040
12. Minami K, Liu S, Liu Y, et al. Inhibitory Effects of Dopamine Receptor D_1 Agonist on Mammary Tumor and Bone Metastasis. *Sci Rep*. 2017;7(1):45686. doi:10.1038/srep45686
13. Albiñana V, Recio-Poveda L, González-Peramato P, Martinez-Piñeiro L, Botella LM, Cuesta AM. Blockade of β2-Adrenergic Receptor Reduces Inflammation and Oxidative Stress in Clear Cell Renal Cell Carcinoma. *Int J Mol Sci*. 2022;23(3):1325. doi:10.3390/ijms23031325
14. Lee D, Ha M, Hong CM, et al. *GABRQ* expression is a potential prognostic marker for patients with clear cell renal cell carcinoma. *Oncol Lett*. 2019;18(6):5731-5738. doi:10.3892/ol.2019.10960
15. Li M, He M, Xu F, et al. Abnormal expression and the significant prognostic value of aquaporins in clear cell renal cell carcinoma. *PLoS One*. 2022;17(3):e0264553. doi:10.1371/journal.pone.0264553
16. David JM, Owens TA, Inge LJ, Bremner RM, Rajasekaran AK. Gramicidin A blocks tumor growth and angiogenesis through inhibition of hypoxia-inducible factor in renal cell carcinoma. *Mol Cancer Ther*. 2014;13(4):788-799. doi:10.1158/1535-7163.MCT-13-0891
17. David JM, Owens TA, Barwe SP, Rajasekaran AK. Gramicidin A induces metabolic dysfunction and energy depletion leading to cell death in renal cell carcinoma cells. *Mol Cancer Ther*. 2013;12(11):2296-2307. doi:10.1158/1535-7163.MCT-13-0445
18. Xie L, Wu S, He R, Li S, Lai X, Wang Z. Identification of epigenetic dysregulation gene markers and immune landscape in kidney renal clear cell carcinoma by comprehensive genomic analysis. *Front Immunol*. 2022;13:901662. doi:10.3389/fimmu.2022.901662
19. Huang CY, Hsueh YM, Chen LC, et al. Clinical significance of glutamate metabotropic receptors in renal cell carcinoma risk and survival. *Cancer Med*. 2018;7(12):6104-6111. doi:10.1002/cam4.1901
20. Bai S, Wu Y, Yan Y, et al. Construct a circRNA/miRNA/mRNA regulatory network to explore potential pathogenesis and therapy options of clear cell renal cell carcinoma. *Sci Rep*. 2020;10(1):13659. doi:10.1038/s41598-020-70484-2
21. Meixner M, Atanasova S, Padberg W, Grau V. Expression of acetylcholine receptors by experimental rat renal allografts. *BioMed Res Int*. 2014;2014:289656. doi:10.1155/2014/289656
22. Sun Y, Li J, Zheng C, Zhou B. Study on polymorphisms in CHRNA5/CHRNA3/CHRNB4 gene cluster and the associated with the risk of non-small cell lung cancer. *Oncotarget*. 2017;9(2):2435-2444. doi:10.18632/oncotarget.23459
23. Chuang YH, Lee CH, Lin CY, et al. An Integrated Genomic Strategy to Identify CHRNB4 as a Diagnostic/Prognostic Biomarker for Targeted Therapy in Head and Neck Cancer. *Cancers (Basel)*. 2020;12(5):1324. doi:10.3390/cancers12051324
24. Zhang B, Wu Q, Xu R, et al. The promising novel biomarkers and candidate small molecule drugs in lower-grade glioma: evidence from bioinformatics analysis of high-throughput data. *J Cell Biochem*. 2019;120(9):15106-15118. doi:10.1002/jcb.28773
25. Alizadeh M, Schledwitz A, Cheng K, Raufman JP. Mechanistic Clues Provided by Concurrent Changes in the Expression of Genes Encoding the M_1 Muscarinic Receptor, β-Catenin Signaling Proteins, and Downstream Targets in Adenocarcinomas of the Colon. *Front Physiol*. 2022;13:857563. doi:10.3389/fphys.2022.857563
26. García-Martín E, Esguevillas G, Serrador M, et al. Gamma-aminobutyric acid (GABA) receptors GABRA4, GABRE, and GABRQ gene polymorphisms and risk for migraine. *J Neural Transm (Vienna)*. 2018;125(4):689-698. doi:10.1007/s00702-017-1834-4
27. Yan L, Gong YZ, Shao MN, et al. Distinct diagnostic and prognostic values of γ-aminobutyric acid type A receptor family genes in patients with colon adenocarcinoma. *Oncol Lett*. 2020;20(1):275-291. doi:10.3892/ol.2020.11573
28. Zhang X, Zhang R, Zheng Y, et al. Expression of gamma-aminobutyric acid receptors on neoplastic growth and prediction of prognosis in non-small cell lung cancer. *J Transl Med*. 2013;11(1):102. doi:10.1186/1479-5876-11-102
29. Lorenzoni PJ, Scola RH, Kay CS, Werneck LC. Congenital myasthenic syndrome: a brief review. *Pediatr Neurol*. 2012;46(3):141-148. doi:10.1016/j.pediatrneurol.2011.12.001
30. Todd EJ, Yau KS, Ong R, et al. Next generation sequencing in a large cohort of patients presenting with neuromuscular disease before or at birth. *Orphanet J Rare Dis*. 2015;10(1):148. doi:10.1186/s13023-015-0364-0
31. Li J, Xu Y, Peng G, et al. Identification of the Nerve-Cancer Cross-Talk-Related Prognostic Gene Model in Head and Neck Squamous Cell Carcinoma. *Front Oncol*. 2021;11:788671. doi:10.3389/fonc.2021.788671
32. Ferguson HJ, Wragg JW, Ward S, Heath VL, Ismail T, Bicknell R. Glutamate dependent NMDA receptor 2D is a novel angiogenic tumour endothelial marker in colorectal cancer. *Oncotarget*. 2016;7(15):20440-20454. doi:10.18632/oncotarget.7812
33. Ma J, Wang P, Huang L, Qiao J, Li J. Bioinformatic analysis reveals an exosomal miRNA-mRNA network in colorectal cancer. *BMC Med Genomics*. 2021;14(1):60. doi:10.1186/s12920-021-00905-2
34. Majumder S, Taylor WR, Foote PH, et al. High Detection Rates of Pancreatic Cancer Across Stages by Plasma Assay of Novel Methylated DNA Markers and CA19-9. *Clin Cancer Res*. 2021;27(9):2523-2532. doi:10.1158/1078-0432.CCR-20-0235
35. Zhang YG, Jin MZ, Zhu XR, Jin WL. Reclassification of Hepatocellular Cancer With Neural-Related Genes. *Front Oncol*. 2022;12:877657. doi:10.3389/fonc.2022.877657
36. Liu S, Zhang Y, Bian H, Li X. Gene expression profiling predicts pathways and genes associated with Parkinson's disease. *Neurol Sci*. 2016;37(1):73-79. doi:10.1007/s10072-015-2360-5
37. Neumann SB, Seitz R, Gorzella A, Heister A, Doeberitz M, Becker CM. Relaxation of glycine receptor and onconeural gene transcription control in NRSF deficient small cell lung cancer cell lines. *Brain Res Mol Brain Res*. 2004;120(2):173-181. doi:10.1016/j.molbrainres.2003.10.021
38. Osman W, Mousa M, Albreiki M, et al. A genome-wide association study identifies a possible role for cannabinoid signalling in the pathogenesis of diabetic kidney disease. *Sci Rep*. 2023;13(1):4661. doi:10.1038/s41598-023-31701-w
39. Turk S, Baesmat AS, Yılmaz A, et al. NK-cell dysfunction of acute myeloid leukemia in relation to the renin-angiotensin system and neurotransmitter genes. *Open Med (Wars)*. 2022;17(1):1495-1506. doi:10.1515/med-2022-0551
40. Roussel E, Kinget L, Verbiest A, et al. C-reactive protein and neutrophil-lymphocyte ratio are prognostic in metastatic clear-cell renal cell carcinoma patients treated with nivolumab. *Urol Oncol*. 2021;39(4):239.e17-239.e25. doi:10.1016/j.urolonc.2020.12.020
41. Quan J, Huang B. Identification and validation of the molecular subtype and prognostic signature for clear cell renal cell carcinoma based on neutrophil extracellular traps. *Front Cell Dev Biol*. 2022;10:1021690. doi:10.3389/fcell.2022.1021690
42. Cordeiro MD, Ilario EN, Abe DK, et al. Neutrophil-to-Lymphocyte Ratio Predicts Cancer Outcome in Locally Advanced Clear Renal Cell Carcinoma. *Clin Genitourin Cancer*. 2022;20(2):102-106. doi:10.1016/j.clgc.2021.10.009
43. Shi Z, Mori-Akiyama Y, Du W, et al. Loss of H2R Signaling Disrupts Neutrophil Homeostasis and Promotes Inflammation-Associated Colonic Tumorigenesis in Mice. *Cell Mol Gastroenterol Hepatol*. 2022;13(3):717-737. doi:10.1016/j.jcmgh.2021.11.003
44. Sun B, Zhao H. The bioinformatics analysis of RIOX2 gene in lung adenocarcinoma and squamous cell carcinoma. *PLoS One*. 2021;16(12):e0259447. doi:10.1371/journal.pone.0259447
45. Sarkans U, Füllgrabe A, Ali A, et al. From ArrayExpress to BioStudies. *Nucleic Acids Res*. 2021;49(D1):D1502-D1506. doi:10.1093/nar/gkaa1062
46. Chen J, Zhou R. Tumor microenvironment related novel signature predict lung adenocarcinoma survival. *PeerJ*. 2021;9:e10628. doi:10.7717/peerj.10628
47. Gordon Smyth [cre a, Yifang Hu [ctb], Matthew Ritchie [ctb], Jeremy Silver [ctb], James Wettenhall [ctb], Davis McCarthy [ctb], Di Wu [ctb], Wei Shi [ctb], Belinda Phipson [ctb], Aaron Lun [ctb], Natalie Thorne [ctb], Alicia Oshlack [ctb], Carolyn de Graaf [ctb], Yunshun Chen [ctb], Mette Langaas [ctb], Egil Ferkingstad [ctb], Marcus Davy [ctb], Francois Pepin [ctb], Dongseok Choi [ctb]. *limma: Linear Models for Microarray Data*.
48. Xie L, Huang G, Gao M, et al. Identification of Atrial Fibrillation-Related lncRNA Based on Bioinformatic Analysis. *Dis Markers*. 2022;2022:8307975. doi:10.1155/2022/8307975
49. Zhang Y, Zheng Y, Fu Y, Wang C. Identification of biomarkers, pathways and potential therapeutic agents for white adipocyte insulin resistance using bioinformatics analysis. *Adipocyte*. 2019;8(1):318-329. doi:10.1080/21623945.2019.1649578
50. Dennis G Jr, Sherman BT, Hosack DA, et al. DAVID: Database for Annotation, Visualization, and Integrated Discovery. *Genome Biol*. 2003;4(5):3. doi:10.1186/gb-2003-4-5-p3
51. Chen L, Zhang YH, Wang S, Zhang Y, Huang T, Cai YD. Prediction and analysis of essential genes using the enrichments of gene ontology and KEGG pathways. *PLoS One*. 2017;12(9):e0184129. doi:10.1371/journal.pone.0184129
52. Kanehisa M. Toward understanding the origin and evolution of cellular organisms. *Protein Sci*. 2019;28(11):1947-1951. doi:10.1002/pro.3715
53. Kanehisa M, Furumichi M, Sato Y, Kawashima M, Ishiguro-Watanabe M. KEGG for taxonomy-based analysis of pathways and genomes. *Nucleic Acids Res*. 2023;51(D1):D587-D592. doi:10.1093/nar/gkac963
54. Kanehisa M, Goto S. KEGG: kyoto encyclopedia of genes and genomes. *Nucleic Acids Res*. 2000;28(1):27-30. doi:10.1093/nar/28.1.27
55. Hemant Ishwaran UBK. *randomForestSRC: Fast Unified Random Forests for Survival, Regression, and Classification (RF-SRC)*. 2023-05-23; Available from: https://www.randomforestsrc.org/https://ishwaran.org/.
56. Zhang X, Shao Z, Xu S, et al. Immune Profiling of Parkinson's Disease Revealed Its Association With a Subset of Infiltrating Cells and Signature Genes. *Front Aging Neurosci*. 2021;13:605970. doi:10.3389/fnagi.2021.605970
57. Ye Y, Dai Q, Qi H. A novel defined pyroptosis-related gene signature for predicting the prognosis of ovarian cancer. *Cell Death Discov*. 2021;7(1):71. doi:10.1038/s41420-021-00451-x
58. Shu W, Wang Z, Zhang W, et al. Identification of EMT-associated LncRNA Signature for Predicting the Prognosis of Patients with Endometrial Cancer. *Comb Chem High Throughput Screen*. 2023;26(8):1488-1502. doi:10.2174/1386207325666221005122554
59. Li H, Li M, Tang C, Xu L. Screening and prognostic value of potential biomarkers for ovarian cancer. *Ann Transl Med*. 2021;9(12):1007. doi:10.21037/atm-21-2627
60. Lin Z, Xu Q, Miao D, Yu F. An Inflammatory Response-Related Gene Signature Can Impact the Immune Status and Predict the Prognosis of Hepatocellular Carcinoma. *Front Oncol*. 2021;11:644416. doi:10.3389/fonc.2021.644416
61. Xu S, Tang L, Liu Z, Luo C, Cheng Q. Hypoxia-Related lncRNA Correlates With Prognosis and Immune Microenvironment in Lower-Grade Glioma. *Front Immunol*. 2021;12:731048. doi:10.3389/fimmu.2021.731048
62. Chen W, Gao C, Liu Y, Wen Y, Hong X, Huang Z. Bioinformatics Analysis of Prognostic miRNA Signature and Potential Critical Genes in Colon Cancer. *Front Genet*. 2020;11:478. doi:10.3389/fgene.2020.00478
63. Tang Y, Guo C, Yang Z, Wang Y, Zhang Y, Wang D. Identification of a Tumor Immunological Phenotype-Related Gene Signature for Predicting Prognosis, Immunotherapy Efficacy, and Drug Candidates in Hepatocellular Carcinoma. *Front Immunol*. 2022;13:862527. doi:10.3389/fimmu.2022.862527
64. Yang P, Liu H, Li Y, et al. Overexpression of *TCERG1* as a prognostic marker in hepatocellular carcinoma: A TCGA data-based analysis. *Front Genet*. 2022;13:959832. doi:10.3389/fgene.2022.959832
65. Song X, Hou L, Zhao Y, Guan Q, Li Z. Metal-dependent programmed cell death-related lncRNA prognostic signatures and natural drug sensitivity prediction for gastric cancer. *Front Pharmacol*. 2022;13:1039499. doi:10.3389/fphar.2022.1039499
66. Yang W, Soares J, Greninger P, et al. Genomics of Drug Sensitivity in Cancer (GDSC): a resource for therapeutic biomarker discovery in cancer cells. *Nucleic Acids Res*. 2013;41(Database issue):D955-D961. doi:10.1093/nar/gks1111
67. Song W, Ren J, Xiang R, Kong C, Fu T. Identification of pyroptosis-related subtypes, the development of a prognosis model, and characterization of tumor microenvironment infiltration in colorectal cancer. *OncoImmunology*. 2021;10(1):1987636. doi:10.1080/2162402X.2021.1987636

ORIGINAL RESEARCH

Targeting Inhibition of Notch 1 Can Promote mTOR Signaling Pathway in Tumor-Related Macrophage to Regulate the Development of Ovarian Cancer

Chunfang Guo, Mmed; Jieyu Mo, Mmed; Xia Liu, Mmed; Yao Chen, Mmed; Lin Liang, Mmed; Huaqiang Li, MD; Li Yang, MD

ABSTRACT

Background • Ovarian cancer is the leading cause of death linked to gynecological cancers. Notch1, as an important component of Notch signaling, plays an important role in a variety of cancers. This study aims to discuss the mechanisms through which Notch 1 influences the development of ovarian cancer.

Methods • To design and establish the short hairpin (sh) RNA for targeting Notch 1, we transfected THP-1 cells (one of the human macrophagic lines). The cells were divided into shRNA negative control (NC) group and the Notch 1 shRNA group. The CoC1 cells and THP-1 cells (human mononuclear macrophages) are co-cultured, which are injected into the nude mice subcutaneously based on proposition. The sizes of tumors and their volumes are observed through HE staining. Flow cytometry is used to sort out macrophages from subcutaneous tumors of nude mice, whose protein-related expression is detected through western blot. Then the NC group and the Notch 1 shRNA group in the co-culture system are treated with PI3K/mTOR Inhibitor-13 sodium (200 nM) for 48h and then co-cultured with human endothelial cell lines HUVEC, CoC1, and THP-1 to test the tube-forming capacity of HUVEC cells in each group to detect the protein-related expression in THP-1 cells using western blot.

Results • It is seen that the Notch 1 shRNA group includes a significantly larger tumor size, decreased relative expression, and the obvious increase of the relative protein expression in p-PI3K, p-mTOR, HIF1α, and VEGF compared with the NC group. Through tube-forming experiments, the Notch1 shRNA group significantly increased the number of HUVEC tubes. However, after the use of PI3K/mTOR Inhibitor-13 sodium, the number of tubes decreased in the NC and Notch1 shRNA groups, and there is no significant discrepancy in comparison to the NC group. The *in vitro* western blotting results indicate no obvious variation of Notch 1's relative protein expression in both the NC group and Notch 1 shRNA group after the use of PI3K/mTOR Inhibitor-13 sodium, while the relative protein expression of p-PI3K, p-mTOR, HIF1α, and VEGF was significantly reduced and there was no significant difference.

Conclusion • This study found that specific knockout of Notch 1 in tumor-associated macrophages will promote the activation of the PI3K/mTOR signaling pathway and the expression of HIF1α and VEGF, thus promoting angiogenesis and the development of ovarian cancer. Thus, this study provides insight into novel prognostic biomarkers and therapeutic targets for the treatment and research of ovarian cancer. (*Altern Ther Health Med.* 2023;29(8):364-369).

Chunfang Guo, Mmed; Jieyu Mo, Mmed; Xia Liu, Mmed; Yao Chen, Mmed; Lin Liang, Mmed; Huaqiang Li, MD; Li Yang, MD; Department of Pathology, Affiliated Banan Hospital of Chongqing Medical University, Chongqing, China.

Corresponding author: Huaqiang Li, MD
E-mail: gcf05162023@163.com
Corresponding author: Li Yang, MD
E-mail: 18883452248@163.com

INTRODUCTION

Ovarian cancer is a malignant tumor caused by ovarian cell differentiation, a common disease in female reproductive system tumors. The onset of ovarian cancer is the most frequent between 50 and 70 years, but about 10 percent of patients diagnosed are under the age of 50 years.[1,2] In particular, most asymptomatic patients are diagnosed at an advanced stage, implying that ovarian cancer is associated with poor prognosis and there is an increasing trend of the incidence of ovarian cancer each year.[3,4] At present, existing immunotherapy for ovarian cancer is not perfect and therefore, it is necessary to provide new ideas for the clinical treatment of ovarian cancer.

Studies have attempted to unravel the mechanism underlying the onset and progression of tumor formation. Tumor-associated macrophages (TAMs) act as a crucial role in the development of tumors. As soon as tumor cells take the

Table 1. Primer Sequences

Notch1-shRNA	Forward	5'-GATCCCCAACATCCAGGACAACATTTCAAGAGAATGTTGTCCTGGATGTTGGTTTTTTCTCGAGG-3'
	Reverse	5'-AATTCCTCGAGAAAAAACCAACATCCAGGACAACATTCTCTTGAAATGTTGTCCTGGATGTGTGGG-3'
shRNA NC	Forward	5'-GATCCTTCTCCGAACGTGTCACGTTTCAAGAGAACGTGACACGTCGGAGAATTTTTTCGAGG-3'
	Reverse	5'-AATTCCTCGAGAAAAAAATTCTCCGAACGTGTCACGTTCTCTTGAAACGTGACACGTCGGAGAG-3'

lead in the tumor microenvironment, tumor-related macrophages are activated and are involved in various stages of cancer progression.[5] Some present studies have already found that blocking the Notch signaling pathway promotes tumor growth in osteosarcoma by affecting the polarization of TAM to the M2 phenotype (anti-inflammatory macrophage).[6]

Notch 1 signaling pathway (an impressive cell signaling pathway) is involved in tumorigenesis including cervical, colon, head and neck, lung, and kidney cancers, as well as pancreatic and breast cancers.[7,8] Besides, it makes an impetus on regulating cell proliferation, differentiation, apoptosis as well as other life processes, [9,10] similar to mTOR signaling pathway which regulates cellular metabolism, proliferation, growth, and survival. It has been attested that aberrant activation of Notch 1 and mechanistic Target of Rapamycin (mTOR) signaling pathways are relevant to many kinds of cancers including ovarian cancer.[11,12] In recent years, researchers have shown that there is an interaction between mTOR signals and Notch 1 which affects the activity of the mTOR pathway by regulating Protein kinase B (PKB or AKT) and phosphatidylinositol 3-kinase (PI3K) pathways.[13,14] and this has a profound impact on tumor differentiation, metastasis, and treatment.[15]

Therefore, we hypothesize that if Notch 1 in tumor-associated macrophages is targeted silencing, the expression of related proteins in the mTOR signaling pathway, as well as HIF1α and VEGF, are affected, affecting angiogenesis and ovarian cancer development. All in all, we demonstrate that specific knockdown of Notch 1 activates the mTOR signaling pathway in tumor-associated macrophages to promote the expression of vascular endothelial growth factor (VEGF) and hypoxia-inducible factor 1α (HIF1α) and stimulate ovarian cancer development.

METHODS

Cell culture

Human-derived macrophages THP-1, ovarian cancer cells CoC1, and human endothelial cells HUVEC from Wuhan, China are cultured in RPMI 1640 complete medium containing 10 percent fetal bovine serum and 1 percent DAB (100 U/mL penicillin and 100 μg/mL streptomycin). All of them are cultured in a constant temperature incubator with 5% CO_2 at 37°C. Subcultures are prepared when the cell confluence reached 80%.

Cell transfection

Notch 1 scrambled negative control short hairpin (sh) RNA (shRNA NC) and Notch1 interfering (Notch1 shRNA) sequences are synthesized by GeneTech (Shanghai) Company Limited. Primer sequences are shown in Table 1.

For formulating double strands after annealing, the sequences of shRNA negative control (NC) or Notch 1 shRNA are cloned into PLVX-shRNA2 predigested with ExoRI and BamHI. The method to transfect shRNA (2 μg) and PLVX vector is to inoculate the THP-1 cell line at the logarithmic growth phase into 24-well plates to adapt the cell density to 4×10^5 pcs/well. Then based on the manufacturer's instructions, Lipofectamine 2000 transfection (Invitrogen; Thermo Fisher Scientific) reagent is used to transfect the plasmid into the THP-1 cell line. Eight hours after transfecting, the cells are incubated at 37°C with 5% CO_2, using RPMI 1640 medium covering 30% ampicillin (1 μg/ml) for transfection. They are incubated in the same environment. After 48 h, the medium is changed for subsequent experiments.

Cell co-culture

CoC1 and HUVEC cells are seeded into transwell chambers and cultured with THP-1 seeded in 24-well plates. After overnight incubation, the medium of the transwell cells and culture plate is removed and new cells are added to the lower cells. Transwell cells are placed in the cell culture plates with a new culture medium, and subsequently tested after 48 hours. Remove the transwell chamber and aspirate the culture medium from the cell culture plate. The cell culture plate is washed twice with PBS and the cells are fixed with 4% paraformaldehyde.

Subcutaneous tumorigenesis experiment in nude mice

In tumorigenesis experiments, CoC1 cells and THP-1 cells after co-culture are injected subcutaneously in each nude mouse into either side of the back of (five-week-old female BALB/c nude mice from Cyagen Biosciences Inc.) in proportion. Tumor size is then tested by measuring the length (L) and width (W) of the tumor with calipers every 3 days, and tumor volume (V) is estimated using the formula $V = 1/2 \times L \times W$.

HE staining

Paraffin sections made from the tumor of nude mice are fully immersed into the dewaxing agent three times and for 30 m each time and dipped in gradient ethanol with concentrations of 100%, 95%, 80%, and 70% for three minutes. After a five-minute soak in hematoxylin solution, the slices are washed in flowing water. Upon differentiation for tens of seconds in 1% hydrochloric acid alcohol, we observe whether the blue cytoplasm sections have disappeared under the microscope and then wash them with running water to terminate differentiation. The sections are washed with running water after 1% ammonia water is used to turn blue for tens of seconds until the nuclei become blue and dip them in eosin solution for 30 seconds along with rinsing the slices with running water. In the end, we dehydrate, make transparent, and seal the slices with environmentally friendly gum.